The Open Construction and Building Technology Journal, 2010, *4*, 64-78

Open Access

Closed-Form Prediction of the Thermal and Structural Response of a Perimeter Column in a Fire

Spencer E. Quiel[1],* and Maria E. M. Garlock[2]

[1]*Hinman Consulting Engineers Alexandria, VA, USA,* [2]*Department of Civil and Environmental Engineering, Princeton University, Princeton, NJ, USA*

Abstract: This paper proposes a simplified closed-form methodology with which to predict the thermal and structural response of steel perimeter columns in high-rise building frames exposed to fire. Due to their orientation in the building compartment, perimeter columns are heated on three sides and will develop a thermal gradient through their cross-sectional depth. Restraint of the thermal expansion associated with this gradient will cause these members to experience a combination of axial load (*P*) and bending moment (*M*), thus acting as beam-columns. At high temperatures, the thru-depth gradient will alter the plastic capacity and mechanical behavior of the perimeter column, leading to plastic *P-M* behavior that is not captured under the assumption of uniform cross-sectional temperature. Simplified methodologies are proposed to calculate the following: (1) the thru-depth temperature distribution that develops due to three-sided heating, (2) the gradient-induced changes in plastic capacity, and (3) the gradient-induced changes in demand (i.e. *P* and *M*). These methodologies are sufficiently simple for use in code-based design and can be implemented via a spreadsheet because they are closed-form. The individual results of each simple methodology as well as their combination are validated against the results of computational thermal and structural analysis, showing good agreement.

Keywords: Fire, beam-column, steel, thermal gradient, performance-based analysis.

INTRODUCTION

Due to the restraint of thermal expansion, many members in a fire-exposed steel building frame will experience a combination of axial load (*P*) and bending moment (*M*), thus acting as beam-columns. In particular, members that develop thermal gradients through their depth due to their orientation in the building frame will experience a combination of *P* and *M* as they encounter restraint to both axial thermal expansion (due to an overall temperature increase) and thermal bowing (due to the thermal gradient) in addition to their gravity loads. The authors have described in detail the changes in plastic *P-M* capacity [1] and *P-M* response [2] experienced by these members, which include perimeter columns (exposed to fire on three sides) and floor beams (whose top face is shielded by the slab). A collaborative experimental study between researchers at Michigan State University and Princeton University successfully demonstrated these behaviors for members loaded in a furnace that simulated the performance of perimeter columns [3]. A resulting numerical study validated the ability of computational models to predict the experimental changes in *P-M* caused by high-temperature thru-depth thermal gradients [3]. This paper addresses the need for performance-based tools to calculate the performance of elements that act as beam-columns and develop thermal gradients through their depth due to fire exposure. Simplified methods are proposed to predict the thru-depth temperature distribution, capacity, and demand induced in beam-columns that are non-uniformly heated.

As shown in Fig. (**1**), performance-based structural-fire analysis is accomplished in two uncoupled phases once a temperature-time relationship representing the fire is selected or calculated: thermal analysis followed by structural analysis. The analyst can select either computational finite element (FE) analysis or closed-form simplified methods to perform these analyses, each having advantages and disadvantages. Computational tools provide a higher level of calculation detail and precision but at a higher cost. Simplified methods can be used more efficiently, but they rely on simplifying assumptions and may not provide the same level of accuracy as computational solutions. Simplified tools that can predict the response of fire-exposed structural members with similar precision as computational methods allows the analyst reap the benefits of using simplified methods without sacrificing accuracy.

In this paper, a simplified methodology is proposed, based on the studies discussed in the aforementioned papers, which explicitly calculates the response of fire-exposed steel beam-columns that develop a thru-depth thermal gradient. The thermal and structural response of these members to fire is obtained via time-series integration by solving closed-form equations at every time step. Emphasis is placed on the case of a wide-flanged perimeter column typical to North American construction, although this method could easily be applied to other member types (i.e. floor beams) or section shapes. The proposed methodology, referred to in this paper as the *simplified member* model, has three primary components: (1) a simplified thermal analysis, (2) a simplified prediction of structural capacity, and (3) a simplified prediction of structural demand. Together, components (2) and (3) comprise the simplified structural analysis shown in Fig. (**1**). The simplified member model can be used to analyze beam-

---

*Address correspondence to this author at Hinman Consulting Engineers Alexandria, VA, USA; Tel: 703-416-6780; Fax: 703-836-4423; E-mail: squiel@hce.com;

$$Q_{in,j} = \frac{P_{p,in,j}\, k_{p,j} \left(T_{fire} - T_{s,j(i-1)}\right)}{d_p} \tag{4a}$$

$$Q_{out,j} = \frac{P_{p,out,j}\, k_{p,j} \left(T_{s,j(i-1)} - T_{ambient}\right)}{d_p} \tag{4b}$$

where j is the fiber number; i denotes the time step; T_{fire} is the fire temperature (°C); $T_{s(i-1)}$ is the temperature of the steel (°C) at the previous time step i-1; k_s and k_p are the thermal conductivity (W/m-K) of the steel and fire protection, respectively; P_u is the perimeter (m) of the unprotected steel surface; h is the convective heat transfer coefficient (W/m^2-K); ε is the relative emissivity; and σ is the Stefan-Boltzmann constant (56.7*10^{-9} W/m^2-K^4). T_{fire} is taken as the fire temperature halfway through the current time step i (i.e. at time $t_{(i-1)} + \Delta t/2$) as an approximation of the fire conditions through the length of the time step [14]. The *in* or *out* subscripts attached to P denote the perimeter that is exposed or unexposed to fire, respectively.

Heat transfer equations for unprotected surfaces (Eq. 3) include both convective and radiative heat transfer. However, these coefficients are not included in the heat transfer equations for protected surfaces. For Eq. 4, it is assumed that the external surface of the insulation has the same temperature as the fire and the internal surface has the same temperature as the steel. The gradient through the thickness of the fire protection between these temperatures is conservatively assumed to be linear, and heat transfer through the insulation is calculated using this gradient in Eq. 4 [15]. The second term in parentheses in Eqs. 1 and 2 also reflects this linear gradient assumption by including a factor of 2 in the denominator (i.e. the temperature of the fire protection equals the average of the fire and steel temperatures). Eurocode replaces the 2 in the denominator of this term with 3 to reduce the conservatism of the linear thermal gradient assumption [5].

Heat transfer between lumped masses a and b (Q_{a-b}) assumes that the linkage between them has a linear thermal gradient:

$$Q_{a-b} = \frac{t_{a-b}\left(T_{s,a(i-1)} - T_{s,b(i-1)}\right)}{y_{a-b}} \left(\frac{k_{s,a} + k_{s,b}}{2}\right) \tag{5}$$

where y_{a-b} is the distance between the centers of gravity of the lumped masses, and t_{a-b} is the thickness of the steel plate that serves as a thermal pathway between them. The value of t_{a-b} is assumed to be t_w for Q_{a-b} between adjacent flange and web lumped masses (e.g. Q_{1-2} and Q_{2-3} in Fig. (**4**(**b**)) and Q_{2-4} in Fig. (**5**(**b**)) and t_f for Q_{a-b} between adjacent flange lumped masses (e.g. Q_{1-2} and Q_{2-3} in Fig. **5**(**b**)). The thermal conductivity between lumped masses is approximated as the average between the thermal conductivity of each, shown as the second term in Eq. 5.

Note that the thermal conductivity (k) and specific heat (c) of both the steel and fire protection in Eqs. 1 through 5 include a subscript corresponding to their lumped mass. Realistically, these material properties are functions of temperature, and they are modeled as such in this methodology. Computational FE solutions use iterative procedures at every time step to calculate the temperature of each fiber. Each fiber's temperature-dependent thermal properties are continuously updated until convergence is achieved and these properties correspond to the fiber's temperature at that time step. To avoid iteration, temperature-dependent thermal properties for steel at the current time step are calculated for each lumped mass according to its steel temperature at the previous time step i-1 ($T_{s(i-1)}$). To calculate updated material properties for the fire protection, the temperature of the fire protection is approximated as the average of T_{fire} at the current time step (as before, calculated for time $t_{(i-1)} + \Delta t/2$) and $T_{s(i-1)}$. This "one-step lag" strategy was successfully used by Gamble [14] to update the temperature-dependent properties of steel and fire protection during analysis of whole cross-sections via a single lumped mass. It will be shown that updating thermal properties according to temperatures from the previous time step provides a sufficiently accurate calculation of steel temperature in each lumped mass fiber as long as the time step remains sufficiently short (i.e. no more than one minute).

SIMPLIFIED PREDICTION OF CAPACITY

A simplified methodology is proposed to predict the plastic capacity of steel beam-columns that develop a thermal gradient through their depth due to non-uniform fire exposure, as in the case of a perimeter column, using the coarse-fiber cross-sectional model described previously. The proposed methodology can be used for beam-columns that develop gradients in the direction of either the strong or weak axis (which thereby induce bending in the same direction). Though not discussed in this paper, buckling must also be considered when calculating the total response of beam-columns to fire. Simple design equations to calculate local buckling strength via stress-based [3,17] or strain-based methods [18], lateral-torsional buckling strength [19], or flexural buckling strength [8] of beam-columns could be added to this procedure to include additional limit states.

Calculating Plastic Capacity

The plastic capacity of a steel cross-section to resist combinations of P and M is calculated using the same procedure proposed by the authors [1], except that this methodology uses the much coarser cross-sectional discretizations shown in Figs. (**2**(**a**) and **3**(**a**)). Temperatures for the lumped masses in this coarse discretization are obtained using the simplified thermal methodology discussed above. Fig. (**6**(**b**)) shows the simplified thermal profile that develops due to three-sided heating of the section shown in Fig. (**6**(**a**)). The yield strength for each fiber, j, is calculated as a function of its temperature. Assuming that the temperature in each fiber has exceeded the value corresponding to a reduction in yield stress, the σ_y profile corresponding to the simplified thermal profile in Fig. (**6**(**b**)) is represented by Fig. (**6**(**c**)) – the larger the temperature, the smaller the σ_y of the steel material. The capacity of the fully yielded section, P_y, is calculated by integrating σ_y of each fiber times its area through the depth of the section, where σ_y has the same sign for all fibers (i.e. all in compression or all in tension as shown in Figs. (**6**(**c**)) and (**g**)). The integration for P shown in [1] can be approximated as a summation over all fibers (i.e. 3 fibers for a strong axis section and 4 fibers for a weak axis section):

$$P = \int_A \sigma_y \, dA = \sum_j \sigma_{y,j} A_j \tag{6}$$

ing the stress at time step *i*, between $\sigma_{p(i)}$ and $\sigma_{y(i)}$. The plastic strain, rather than the maximum stress level, describes the complete stress-strain history as the steel temperature changes [21]. As the material unloads from point ***A***, it travels the path ***ABC***, which has a non-zero value of $\varepsilon_{pl(i)}$ - the material no longer passes through the origin at point ***O***. The simplified model unloads with elastic modulus $E_{(i)}$ over a stress range of $2\beta_p$ (where β_p is equal to $\sigma_{p(i)}$) regardless of the value of $\varepsilon_{pl(i)}$ [21], and the portion of load path ***ABC*** for negative stresses rejoins the original material model via the tangent stiffness $E_{t(i)}$. Calculations using the Eurocode model when plastic strains have developed are more complicated; for example, the construction of negative-stress portion of pathway ***ABC*** requires the use of several non-linear branches to rejoin the original material model ***AOC*** [21]. The simplified model is therefore used as a simpler alternative.

Note that the tri-linear model will estimate a larger $\varepsilon_{pl(i)}$ for a given value of $\sigma_{(i)}$ than the Eurocode model. Likewise, strains at each time step, $\varepsilon_{(i)}$, for a given value of $\sigma_{(i)}$ between $\sigma_{p(i)}$ and $\sigma_{y(i)}$ will also be larger when calculated with the simplified model (see Fig. **9**). The methodology proposed in this paper applies an adjustment factor to account for this error. The magnitude of this adjustment factor will be discussed later in this paper, and the effectiveness of using the simplified material model in this fashion will be confirmed via comparison to computational results. Experimental validation of this adjustment factor is also provided in [3].

The total strain of every fiber in the beam-column cross-section (ε_{total}) is comprised of the mechanical strain ($\varepsilon_{\sigma,j}$) plus the thermal strain ($\varepsilon_{T,j}$), which equals the coefficient of thermal expansion times the change in the fiber's temperature ($\alpha\Delta T_j$). Note that ε_{total} does not have a subscript *j* representing the fiber. For the column shown in Fig. (**8**(**a**)), the rotation of each end is restrained, and therefore the curvature is zero and ε_{total} will be constant through the section depth since all fibers translate uniformly in the vertical direction. To calculate the *P-M* response of the coarsely discretized cross-section, the secant modulus, $E_{s,j}$, is used as a generalized description of each fiber's stiffness [22,23], as shown in Fig. (**9**) for time step *i*:

$$E_{s,j} = \frac{\sigma_j}{\varepsilon_{\sigma,j}} \tag{8}$$

When $\sigma_j < \sigma_{p,j}$, $E_{s,j}$ equals the modulus of elasticity, reduced as a function of temperature ($E_j = E_{20}k_{E,T,j}$). Once $\sigma_j > \sigma_{p,j}$, $E_{s,j}$ does not represent the true stiffness of each fiber but rather a relative measure of stiffness between fibers which will be shown to be sufficient for predicting structural response. Fig. (**9**) shows that the simplified steel material model underestimates E_s compared to the Eurocode model. As for the overestimation of strain, this error will be accounted for via an adjustment factor when demand is calculated.

Note that $E_{s,j}$ is a function of both the temperature at time step *i* and the corresponding stress-strain state of fiber *j*. Computational FE analysis tools use iterative methods that update the value of $E_{s,j}$ at every iteration so that it corresponds directly to the column's temperature and stress-strain state at that time step. To avoid iteration, the proposed methodology calculates the values for $E_{s,j}$ at time step *i* using the stress and strain from time step *i-1*, similar to the "one-step lag" strategy used to update temperature-dependent material properties in the simplified thermal analysis outlined in Section 3 [14]. It will be shown later in this paper that this simplification provides reasonably accurate results.

Calculating *P*

The magnitude of axial load *P* at time step *i* is calculated with the following expression, which accounts for the resistance of the vertical spring in Fig. (**8**(**a**)) to vertical thermal expansion:

$$P = P_o + \left(\varepsilon_{total} - \varepsilon_o\right)k_{spring}L \geq P_o \tag{9}$$

P_o and ε_o represent the initial applied axial load and initial strain experienced by the column, and *L* is the length of the column as shown in Fig. (**8**(**a**)). Recall that ε_{total} equals the sum of $\varepsilon_{T,j}$ and $\varepsilon_{\sigma,j}$ – its value describes the total axial elongation of the column in response to heating and is the same for every fiber at each time step. The total strain is adjusted by ε_o so that only upward displacements from the initially loaded position can induce an increase in *P*. For the same reason, the minimum magnitude of *P* in Eq. 9 is restricted to P_o.

Calculating M_T

To calculate M_T at time step *i*, the analyst needs to determine the mechanical (or stress-related) strains induced via resistance to thermal curvature at every fiber *j* ($\varepsilon_{\sigma,T,j}$). Mechanical strain $\varepsilon_{\sigma,j}$ is comprised of $\varepsilon_{\sigma,T,j}$ plus $\varepsilon_{\sigma,P,j}$, which is the mechanical strain induced by applied load *P*. The authors have previously shown that M_T can be calculated based on $\varepsilon_{T,j}$, $E_{s,j}$, A_j, and y_j only [2]. As mentioned previously, $E_{s,j}$ is calculated according to σ_j and $\varepsilon_{\sigma,j}$ from time step *i-1*. Assuming that all fibers are in equilibrium and that the column cross-section remains horizontal (i.e. ε_{total} is constant for all fibers), M_T is calculated with the following expression:

$$M_T = \eta\sum_j \varepsilon_{\sigma,T,j}E_{s,j}y_jA_j = \eta\sum_j\left(\frac{\sum \varepsilon_{T,j}E_{s,j}A_j}{\sum E_{s,j}A_j} - \varepsilon_{T,j}\right)E_{s,j}y_jA_j \tag{10}$$

Adjustment factor η is included in Eq. 10 to address the overestimation of strain (and subsequent underestimation of $E_{s,j}$) that occurs when the simplified trilinear material model for steel is used instead of the Eurocode model (see Fig. **9**). In the course of this study, the authors have found that using a value of $\eta = 0.75$ produces good agreement with analysis results of computational models that account for realistic material, geometric, and thermal non-linearities as will be discussed later in this paper.

Calculating M_{P*e}

To calculate M_{P*e} at time step *i*, the position of the effective centroid (y_{EC}) must be calculated. The effective centroid represents the center of stiffness in a steel cross-section – it is the location through which the axial load must be applied to produce pure axial stress with no bending. The effective centroid of a cross-section with a uniform temperature profile will coincide with its geometric centroid. Assuming that the maximum temperature is high enough to cause a reduction in stiffness (i.e. $E_{s,j}$), y_{EC} for a cross-section with a non-uniform temperature profile will migrate toward to cooler parts of the cross-section with higher stiffness. Using a simi-

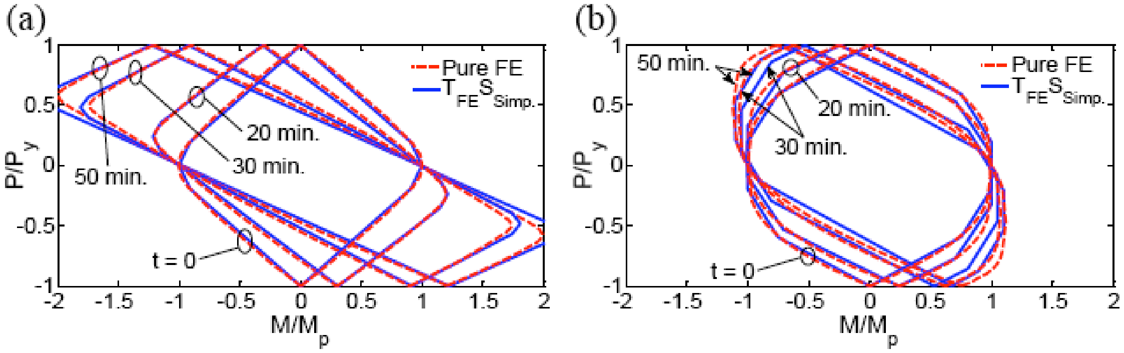

Fig. (16). Plots of plastic *P-M* capacity envelopes for (**a**) 1MP-S and (**b**) 1MP-W at various times during fire exposure.

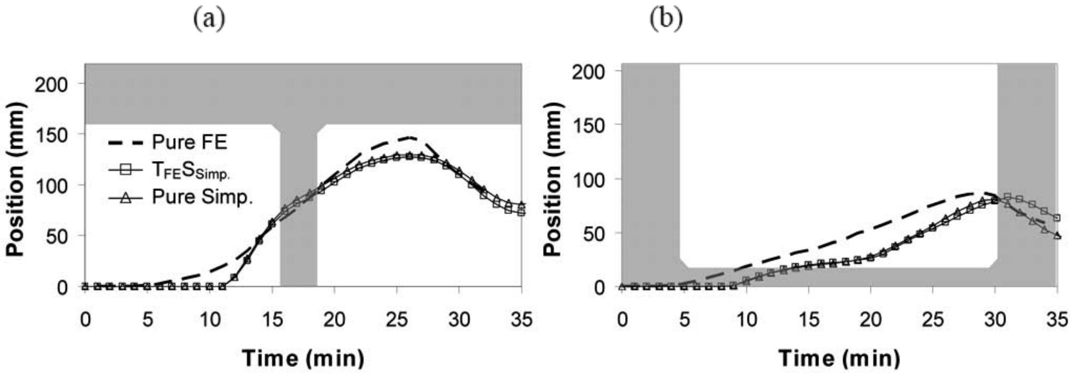

Fig. (17). Plot of y_{EC} for (**a**) 1MP-S and (**b**) 1MP-W.

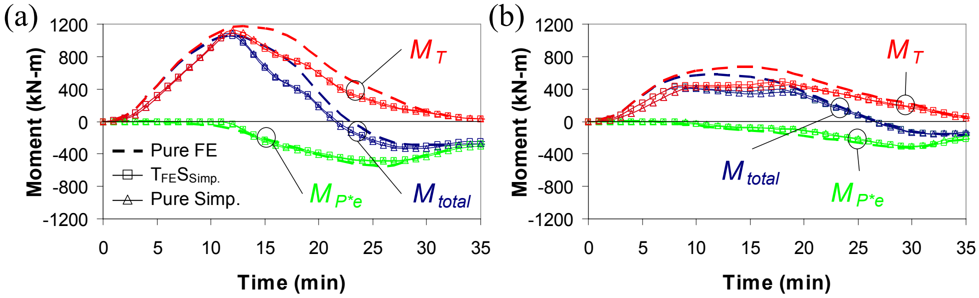

Fig. (18). Plot of moment components for (**a**) 1MP-S and (**b**) 1MP-W.

computationally derived capacity envelopes marked "Pure FE" were derived using the methods developed by the authors [1] for thermal profiles obtained via FE thermal analysis of the discretized cross-sections shown in Fig. (**13**). The envelopes corresponding to simplified structural analysis solutions ($T_{FE}S_{Simp}$) were constructed according to the method outlined previously using the coarse-fiber thermal profiles. The plots in Fig. (**16**) show close agreement between the FE and simplified predictions of plastic capacity.

Combined P-M Demand

Figs. (**17**(**a**) and (**b**)) show the position of the effective centroid (y_{EC}) for columns 1MP-S and 1MP-W, respectively, calculated via FE and simplified structural analysis. The shaded region in each plot represents the cooler half of the wide-flanged cross-section and is used to illustrate the position of y_{EC} relative to the section's depth. Initially, the effective centroid coincides with the geometric centroid (at position = 0) and then migrates into the cooler half of the section due to the thermal gradient. The FE and simplified structural analyses provide similar predictions of y_{EC}. Figs. (**18**(**a**) and (**b**)) show plots of the total moment, M_{total}, experienced by each 1MP column during fire exposure as well as its two components, M_T and M_{P*e}. Initially, the columns develop positive M_T because the rotationally rigid boundary conditions restrict thermal bowing, and M_{total} equals M_T since y_{EC} still coincides with the geometric centroid. When y_{EC} migrates toward the cooler half of the section, negative M_{P*e} is generated. At this time, M_{total} peaks and begins to reverse direction as the rate of increase of M_{P*e} becomes larger than the rate of increase of M_T. Eventually, M_{P*e} becomes larger than M_T, and M_{total} reverses sign. Good agreement is again shown between the FE and simplified predictions.

Predicting Failure

Fig. (**19**) shows plots of *P* and *M* for the FE and simplified structural analyses of each validation case at the time of failure. The values of *P* and *M* are normalized by their corre-

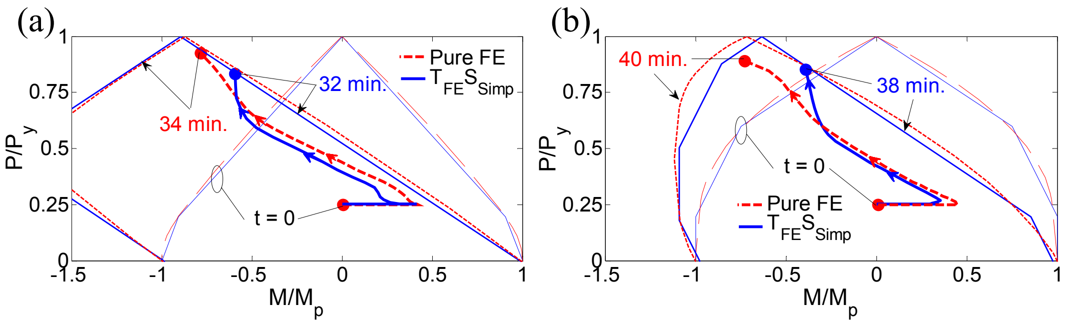

Fig. (19). Plots of normalized *P-M* performance for (**a**) 1MP-S and (**b**) 1MP-W.

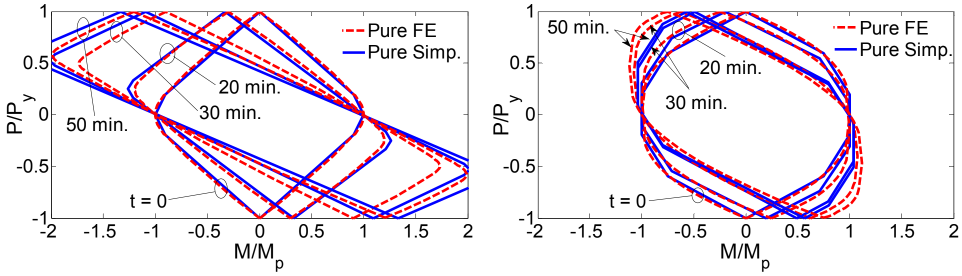

Fig. (20). Plots of plastic *P-M* capacity envelopes for (**a**) 1MP-S and (**b**) 1MP-W at various times during fire exposure.

sponding yield strength (P_y) and plastic moment (M_p) at every time step according to Eq. 12. Each plot also includes the normalized plastic *P-M* capacity envelopes for $t = 0$ (i.e just prior to fire exposure) and for the temperature distribution at the time of failure. Since moment is constant along the length of the column (Fig. **8**), the plotted path of *P* and *M* therefore describes the ratio of demand to capacity for the entire column.

The path of *P-M* combinations during fire exposure progresses from the point marked $t = 0$ to a point marked with a specific time of failure. The *P-M* behavior of both validation cases in Fig. (**19**) shows good agreement between the FE and simplified structural analyses. The plots of normalized *P-M* for all analyses show both the initial increase in positive moment (M_T) and the moment reversal due to increasing negative values of M_{P*e}. The significant increase in axial load ratio P/P_y for each case was caused primarily by a decrease in P_y. The magnitude of M/M_p was also amplified by a simultaneous decrease in plastic capacity. The coupled effects of increasing load and decreasing capacity push the section closer to its plastic capacity until the path of normalized *P* and *M* reaches the capacity envelope and analysis ends, indicating that the section has fully yielded.

Table **1** summarizes the times at which full section yield occurs in the FE analyses using fiber-beam elements in SAFIR and the solution obtained using the simplified structural analysis methodology. The FE and simplified structural analyses show good agreement in predicting the time at which each column experienced an intersection of capacity and demand as illustrated in Fig. (**19**), and the simplified structural analyses consistently provided conservative predictions of performance. This agreement, which is a product of the close agreement between the individual predictions of capacity and demand, confirms that the closed-form simplified structural analysis methodology can effectively predict the changes in capacity and demand experienced by perimeter columns under fire (which develop a thru-depth thermal gradient and act as beam-columns).

Table 1 – Recorded times (in minutes) to column failure.

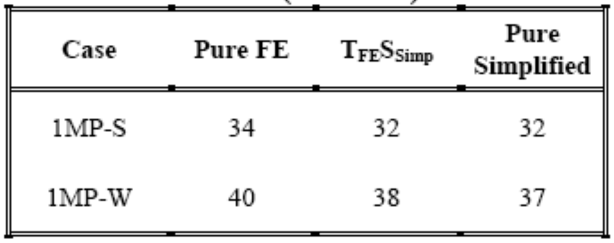

Case	Pure FE	$T_{FE}S_{Simp}$	Pure Simplified
1MP-S	34	32	32
1MP-W	40	38	37

Validating the Combination of Simplified Thermal and Structural Analysis

The results of simplified thermal analysis can be used to construct the coarse-fiber temperature profile needed as input for simplified structural analysis. This combination, (i.e. the Pure Simplified solution in Fig. **1**) provides a closed-form prediction of the total response of a perimeter column to fire exposure. The Pure Simplified solutions for both validation cases use the temperatures marked T_{Simp} in Fig. (**14**) as input for simplified structural analysis. The results of these simplified analyses are compared to the solutions using FE structural analysis (Pure FE) to validate the accuracy of the combined thermal and structural simplified analysis methodology.

Fig. (**20**) shows reasonable agreement of the plastic *P-M* capacity envelopes predicted by the Pure Simplified solution and the FE structural analyses for both validation cases at several times during fire exposure. Variation between the simplified and computational/experimental temperatures (see Fig. **14**) translates into slightly more variation in the shape of the plastic *P-M* envelopes in Fig. (**20**) as compared to Fig. (**16**) (i.e. the $T_{FE}S_{Simp}$ solutions). Figs. (**17** and **18**) show that the predictions of demand are less sensitive to variations in

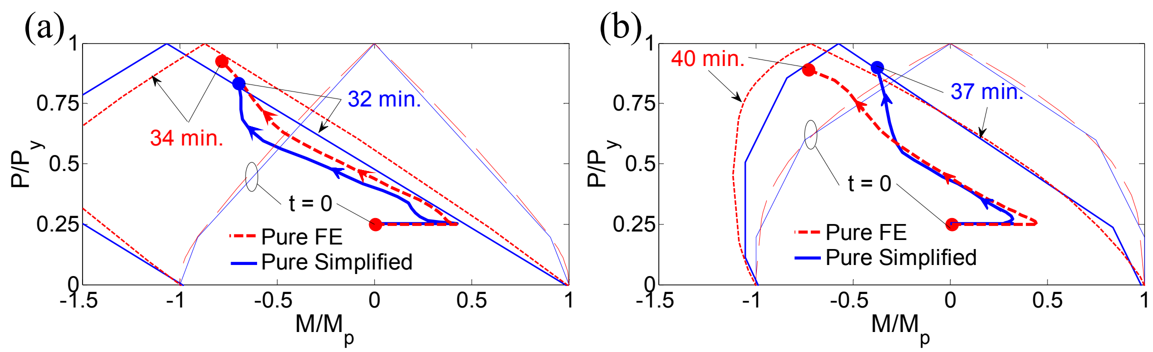

Fig. (21). Plots of normalized *P-M* performance for (**a**) 1MP-S and (**b**) 1MP-W.

predicted temperature because all solutions using simplified structural analysis (i.e. the $T_{FE}S_{Simp}$ and Pure Simplified solutions) are similar and agree well with those using FE structural analysis (Pure FE). Fig. (**21**) shows the time and pathway with which the normalized *P-M* points reach the plastic capacity envelope show good agreement between the Pure Simplified solutions and those predicted via FE structural analysis. Table **1** shows that the analyses all predicted similar times to failure. These comparisons demonstrate that the combination of the simplified thermal and structural analyses can be used to accurately calculate the fire-exposed response of steel perimeter column using only closed-form expressions.

SUMMARY AND CONCLUSIONS

A simplified methodology is proposed to calculate the response of steel beam-columns that develop a thermal gradient through their depth due to non-uniform fire exposure. The current version of the methodology focuses on the performance of wide-flanged perimeter columns under fire, although it could be adapted for the analysis of other sections shapes or beam-column cases (such as floor beams). The expressions developed for simplified time-series integration are closed-form, allowing the user to explicitly calculate thermal and structural response at each time step without using iterative or computational methods. The proposed methodology, referred to as the *simplified member* model, has three primary components, each of which was outlined in detail in this paper: (1) a simplified thermal analysis, (2) a simplified prediction of capacity, and (3) a simplified prediction of demand. Together, components (2) and (3) comprise a simplified structural analysis. Both the simplified thermal and structural analyses subdivide the cross-section of the beam-column into a small number of coarse fibers. Based on previous work by Ghojel and Wong [16], heat transfer between these fibers (represented as lumped masses) and the surrounding environment can be calculated to obtain a non-uniform temperature distribution about either the strong or weak axis. The capacity and demand of the column is calculated via summation of the strength, stress, and strain of each fiber in response to temperature and loading and is compared at every time step. The results of these analyses can be combined to provide a closed-form prediction of the total response of a perimeter column under fire.

Two perimeter column prototypes were used to validate our simplified thermal and structural analysis methodologies against computational results. These methodologies were also validated against experimental results [3], although not discussed in this paper. Coarse-fiber temperatures calculated for each validation case via simplified thermal analysis showed good agreement with the results of FE thermal analysis. The simplified structural analyses (with thermal FE inputs) provided similar predictions of capacity and demand, as well as the mode and time to failure, as the FE models. Both the thermal and structural simplified methodologies were combined to obtain a pure simplified solution that did not rely on any FE analyses. These pure simplified solutions also showed good agreement with the results of FE structural analysis.

The simplified methodologies proposed in this paper offer a simple, closed-form alternative to computational FE analysis to calculate the response of perimeter columns to fire. The good agreement of simplified predictions with computational and experimental results indicates that simple methods can be used to effectively and efficiently predict the response of beam-columns that develop thermal gradients through their depth. The simplified methodology can be implemented in a spreadsheet or other non-iterative mathematical algorithm and has potential as a useful tool for the performance-based design of steel beam-columns under fire. The closed-form calculations presented in this paper can be incorporated into a performance-based design procedure for steel perimeter columns, which is currently being developed by the authors [3].

ACKNOWLEDGEMENTS

The research presented in this paper is based on work that is co-sponsored by the National Science Foundation (NSF) (under grant number CMMI-0652282) and the National Institute of Standards and Technology (NIST) (under grant number 60NANB7D6121). Dr. Quiel's involvement with this research project began while on appointment as a U.S. Department of Homeland Security (DHS) Fellow under the DHS Scholarship and Fellowship Program, which is administered by the Oak Ridge Institute for Science and Education (ORISE) for DHS through an interagency agreement with the U.S Department of Energy (DOE). ORISE is managed by Oak Ridge Associated Universities under DOE contract number DE-AC05-00OR22750. All opinions, findings, and conclusions expressed in this dissertation are the authors' and do not necessarily reflect the policies and views of the DHS, DOE, ORISE, NSF, or NIST.

REFERENCES

[1] M. E. M Garlock and S. E. Quiel, "Plastic axial load - moment interaction curves for fire-exposed steel sections", *Journal of Structural Engineering* (ASCE), vol. 134, pp. 874-880, 2008.

[2] M. E. M. Garlock, and S. E. Quiel, "Mechanics of wide-flanged steel sections that develop thermal gradients due to fire exposure", *International Journal of Steel Structures* (KSSC), vol. 7, pp. 153-162, 2007.

[3] S. E. Quiel, "*Behavior and Analysis of Fire-Exposed Steel Beam-Columns that Develop Thermal Gradients*", PhD Thesis, Princeton University: Princeton, NJ, USA, June 1, 2009.

[4] R. G. Gann, ed., *NIST NCSTAR 1: Final Report of the National Construction Safety Team on the Collapse of the World Trade Center Twin Towers,* Gaithersburg, MD: National Institute of Standards and Technology (NIST), 2005.

[5] CEN, *Eurocode 3: Design of Steel Structures, Part 1.2: General Rules – Structural Fire Design (ENV 1993-1-2:2001)*, Brussels: European Committee for Standardization (CEN), 2001.

[6] AISC, *Steel Construction Manual*, 13th Ed., Chicago: American Institute of Steel Construction (AISC), 2005.

[7] J. Takagi and G. G. Deierlein, "Strength design criteria for steel members at elevated temperatures", *Journal of Constructional Steel Research*, vol. 63, pp. 1036-1050, 2007.

[8] M. Knobloch, M. Fontana and A. Frangi, "Steel beam-columns subjected to fire", *Steel Construction*, vol. 1, pp. 51-58, 2008.

[9] N. Lopes, L. Simões da Silva, P. M. M. Vila Real and P. Piloto, "New proposals for the design of steel beam-columns in case of fire, including a new approach for the lateral torsional buckling", *Computers and Structures*, vol. 82, pp. 1463-1472, 2004.

[10] W. Skowronski, "Buckling fire endurance of steel columns", *Journal of Structural Engineering* (ASCE), vol. 119, pp. 1712-1732, 1993.

[11] Z. F. Huang and K. H. Tan, "Analytical fire resistance of axially restrained steel columns", *Journal of Structural Engineering* (ASCE), vol. 129, pp. 1531-1537, 2003.

[12] G. Q. Li, W. Y. Wang and S. W. Chen, "A simple approach for modeling fire-resistance of steel columns with locally damaged fire protection", *Engineering Structures*, vol. 31, pp. 617-622, 2009.

[13] A. S. Usmani, J. M. Rotter, S. Lamont, A. M. Sanad and M. Gillie, "Fundamental principles of structural behaviour under thermal effects", *Fire Safety Journal*, vol. 36, pp. 721-744, 2001.

[14] W. L. Gamble, "Predicting protected steel member fire endurance using spread-sheet programs", *Fire Technology*, vol. 25, pp. 256-273, 1989.

[15] A. H. Buchanan, *Structural Design for Fire Safety*, Chichester, UK: John Wiley & Sons, 2002.

[16] J. I. Ghojel and M. B. Wong, "Three-sided heated of I-beams in composite construction exposed to fire", *Journal of Constructional Steel Research*, vol. 61, pp. 834-844, 2005.

[17] CEN, *Eurocode 3: Design of Steel Structures, Part 1.5: Plated Structural Elements (ENV 1993-1-5:2004)*, Brussels: European Committee for Standardization (CEN), 2004.

[18] M. Knobloch and M. Fontana. "Strain-based approach to local buckling of steel sections subjected to fire", *Journal of Constructional Steel Research*, vol. 62, pp. 44-67, 2006.

[19] P. M. M. Vila Real, N. Lopes, L. Simões da Silva, P. Piloto and J. M. Franssen, "Numerical modelling of steel beam-columns in case of fire – comparisons with Eurocode 3", *Fire Safety Journal*, vol. 39, pp. 23-39, 2004.

[20] M. E. M. Garlock and S. E. Quiel, "The behavior of steel perimeter columns in a high-rise building under fire", *Engineering Journal* (AISC), vol. 44, pp. 359-372, 2007.

[21] J. M. Franssen, "The unloading of building materials submitted to fire," *Fire Safety Journal*, vol. 16, pp. 213-227, 2009.

[22] J. A. El-Rimawi, I. W. Burgess and R. J. Plank, "The analysis of semi-rigid frames in fire – a secant approach", *Journal of Constructional Steel Research*, vol. 33, pp. 125-146, 1995.

[23] I. W. Burgess, J. A. El-Rimawi and R. J. Plank, "Analysis of beams with non-uniform temperature profile due to fire exposure", *Journal of Constructional Steel Research*, vol. 16, pp. 169-192, 1990.

[24] J. M. Franssen, "SAFIR: A thermal/structural program for modeling structures under fire", *Engineering Journal* (AISC), vol. 42, pp. 143-158, 2005.

Received: June 25, 2009 Revised: October 10, 2009 Accepted: October 12, 2009

© Quiel and Garlock; Licensee *Bentham Open*.

This is an open access article licensed under the terms of the Creative Commons Attribution Non-Commercial License (http://creativecommons.org/licenses/by-nc/3.0/) which permits unrestricted, non-commercial use, distribution and reproduction in any medium, provided the work is properly cited.